Kapvik Manipulator

Antonio Maria Corsetti, Roberto Lucchesi

January 2024

1 Introduction

The Kapvik microRover is a smart, reconfigurable all-terrain multimission microRover prototype that was developed to address the challenges of planetary exploration and sample acquisition. It consists a mobile platform, a robotic mast and a number of sensor for surface exploration and sample retrieval. The robotic mast can perform sample acquisition and transfer for storage as well as assist the microRover in navigation and inspection. To satisfy the stowage and navigation constrains a mechanism is built in order to provide stability and enable self-locking and unlocking of the robotic mast. The goal of this report is to address seven tasks, namely:

1. Model the Kapvik robotic arm by using the Modified or Standard Denavit-Hartenberg formulation.
2. Implement forward and inverse kinematics algorithms.
3. Determine the Jacobian.
4. Determine the dynamical equations.
5. Determine the trajectory of the end-effector that enables:
   a. Smooth transition between stowage and navigation configurations.
   b. Sample retrieval and transfer on the rover platform starting from the stowage configuration.
6. Simulate the robotic arm control for the trajectory determined in 5.a from the stowage to the navigation configuration.
7. Simulate the robotic arm control for the trajectory determined in 5.b.

2 Mechanical Design

The robotic arm consists of four rotary joints and a scoop. The upper arm and forearm links are designed as slim pipes with an outer diameter of 40 mm and a shell thickness of 2 mm. The lengths of the upper arm and forearm are selected as 0.46 and 0.44 m, respectively. Each joint is composed of a motor/gear assembly, a harmonic drive, and the associated electronic parts

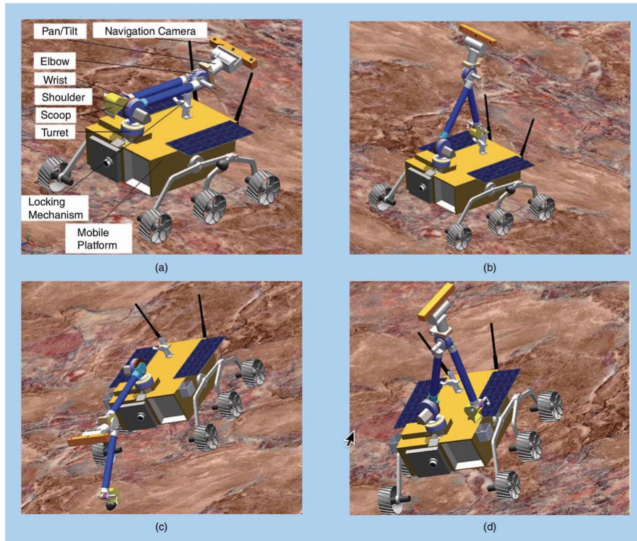

Figure 1: The four main configuration of the Kapvik microRover

2.1 Robotic Arm

The Kapvik robot arm is design in order to satisfy four main configurations as shown in Figure 1

1. stowage configuration (a)
2. navigation configuration (b)
3. sample retrieval configuration (c)
4. sample transfer configuration (d)

The stowage configuration is designed to allow the robotic arm to fold on top of the mobile platform for the convenience of transportation, in the navigation configuration, the robotic mast locks itself and forms a solid triangle to provide steady support for the navigation camera. The sample retrieval configuration enables a ground sampling and the acquired sample is transferred to a container for later analysis.

3 Modeling of the Kapvik robotic arm using the MDH formulation

To model the Kapvik robotic arm using the MDH formulation we need to define several parameters, after we defined the link frame as rigidly attached to the link.

i	α_{i-1}	a_{i-1}	d_i	q
1	0	0	0	q_1
2	$\frac{\pi}{2}$	0	0	q_2
3	0	L1	0	q_3
4	0	L2	0	q_4

Table 1: Table of MDH parameters

- a_i is the link length
- α_i is the twist angle
- d is the link offset, the distance along the common axis from one link to the next
- θ_i is the amount of rotation about the common axis between the two links. (Also referred as q)

One should notice how the the variable is d if we are dealing with prismatic joint, and θ is the joint is revolute. Since our manipulator is made up only of revolute joint the variable will be θ or q. Therefore the modelling of out robotic arm will be as shown in Table 1

We define the limit angles for each joint:

Joint	Limit angles
1	-160,100
2	-90,90
3	-150,110
4	-90,5

Table 2: Limit angles for each joint, taken in degree

We impose an offset from the conventional deployed arm reference frame of q_{off} = [0 90 0 0] to allow the arm to perform all configurations respecting joint limits

3.1 Forward Kinematics

The direct Kinematics is defined by the equation

$$\boldsymbol{X} = \boldsymbol{f}(q) \tag{1}$$

where $\boldsymbol{q} = [q1, q2, q3, q4]$ are the four joint positions, angles, $\boldsymbol{X} = [x, y, z, \phi, \theta, \psi]$ is the position and orientation (Roll, Pitch and Yawn) of end effector, and $\boldsymbol{f}$ is the modeling of the geometry of the manipulator. Therefore, by knowing the joint angles we can define the pose of the end effector $\boldsymbol{X}$. To do so we define the homogeneous transformation from one link to another using the matrix:

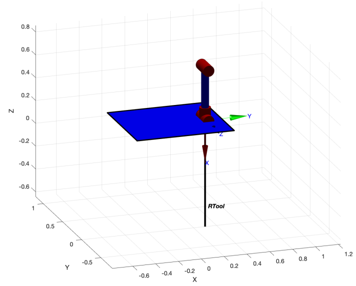

Figure 2: $\boldsymbol{q} = [0\ 0\ 0\ 0]$

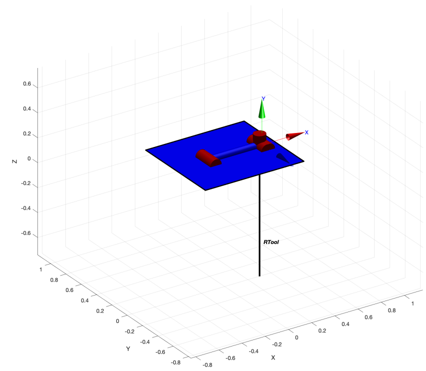

Figure 3: Stowage

$$T_i^{i-1} = R_x(\alpha_{i-1})D_x(a_{i-1})R_z(q_i)D_z(d_i) \tag{2}$$

where the matrices R_x, R_z are rotations along the $\hat{X}$ and $\hat{Z}$ axis, and in similar fashion D_x, D_z are translation matrices. So by consulting the MDH table and iterating this matrix from first to last joint we obtain the homogeneous transformation: $T_0^N = T_1^0 T_2^1 ... T_N^{N-1}$ which allows to know the pose on the end effector with respect to the base of the manipulator.

3.2 Inverse Kinematics

Now we present the inverse problem: starting from the pose of the end effector we wish to know what are the joint coordinates $\vec{q}$ that give such pose. So:

$$\boldsymbol{q} = \boldsymbol{f}^{-1}(\boldsymbol{X}) \tag{3}$$

It is important to notice how the solution is not unique and only exhist if the desired pose lies in the manipulator's workspace. Two main strategies are adopted in order to solve for the inverse Kinematics:

- Numerical solution
- Closed form solution

The Kapvik's manipulator arm is made up by 4 joints, 3 that shares the same rotation axis and one whose rotation axis is tilted by $\alpha = \pi/2$, therefore by analyzing the geometry of the manipulator is possible to achieve a closed solution.

3.3 Closed form solution

The joint is under actuated, because we have 4 degrees in joint space and 6 degrees in cartesian space. To derive the inverse kinematic, we first need to isolate the coordinates of our interest. In this case, we choose to look for [x, y, z, ϕ], position and pitch of the end effector, and discard the other 2 degrees of freedom of roll and yaw rotations of the end effector. In the off plane (x-y) we have:

$$
\begin{aligned}
x &= r_{x,y} \cos q_1 \\
y &= r_{x,y} \sin q_1
\end{aligned}
$$

that leads to the determination of the joint variable q_1 by:

$$\tan q_1 = \frac{y}{x} \tag{4}$$

For the in-plane (x'-z) we rotate the reference frame by the azimuthal angle, so we have:

$$
\begin{aligned}
x' &= \sqrt{x^2 + y^2} \\
x' &= L_1 \cos q_2 + L_2 \cos(q_2 + q_3) \\
y &= L_1 \sin q_2 + L_2 \sin(q_2 + q_3)
\end{aligned}
$$

it is possible to isolate the cosine component of q_3, by means of the equation:

$$\cos(q_3) = \frac{x^2 + z^2 - (L_1^2 + L_2^2)}{2L_1L_2} \tag{5}$$

and then using the trigonometric identity to calculate the sine component $\sin(q_3) = \sqrt{1 - \cos(q_3^2)}$ we can obtain q_3:

$$q_3 = \arctan(\frac{\sin(q_3)}{\cos(q_3)}) \tag{6}$$

remembering that if $\cos q_3 > 1$ or $\cos q_3 < -1$ the desired pose is out of reach. With the knowledge of q_3 it is possible to compute q_2. Defining:

$$
\begin{aligned}
k_1 &= L_1 + L_2 \cos(q_3) \\
k_2 &= L_2 \sin(q_3)
\end{aligned}
$$

we can rewrite the equations:

$$
\begin{aligned}
x' &= k_1 \cos q_2 - k_2 \sin q_2 \\
z &= k_1 \sin q_2 + k_2 \cos q_2
\end{aligned}
$$

we get:

$$q_3 = \arctan(\frac{y}{x}) - \arctan(\frac{k2}{k1}) \tag{7}$$

And now for the last joint:

$$q_4 = \arctan(\frac{\sin\phi}{\cos\phi}) - (q_2 + q_3) \tag{8}$$

So we end up with 4 joint angles that completely solve the inverse kinematic problem.

3.4 From Cartesian Coordinates to Joint Coordinates

Having defined the inverse kinematics, we can give in input several cartesian coordinates that are mainly the position of the tool with respect the base of the manipulator, in order to get the joint variables associated to the poses we want to follow the trajectory. We set the origin of the reference frame at the base of the manipulator.

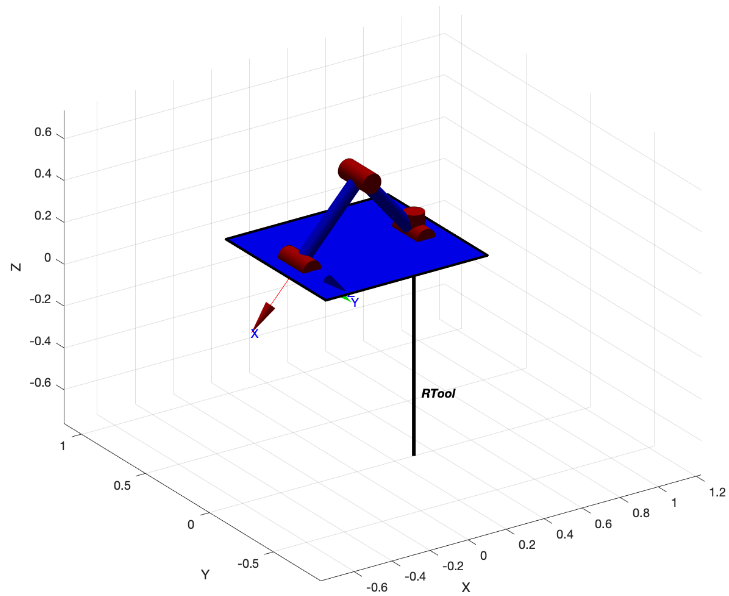

Figure 4: Navigation
$\boldsymbol{x}_{nav}$ = [-0.6 0 0 0]
$\boldsymbol{q}_{nav}$ = [0 40 -83.58 0]

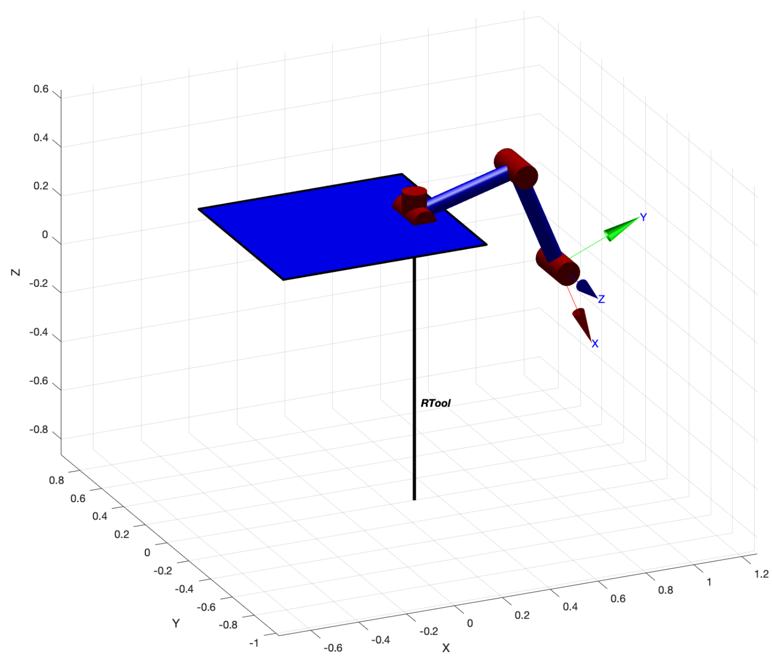

Figure 5: Sample Retrieval
$\boldsymbol{x}_{sam}$ = [0.6 0 -0.31 0]
$\boldsymbol{q}_{sam}$ = [0 -74.81 97.22 0]

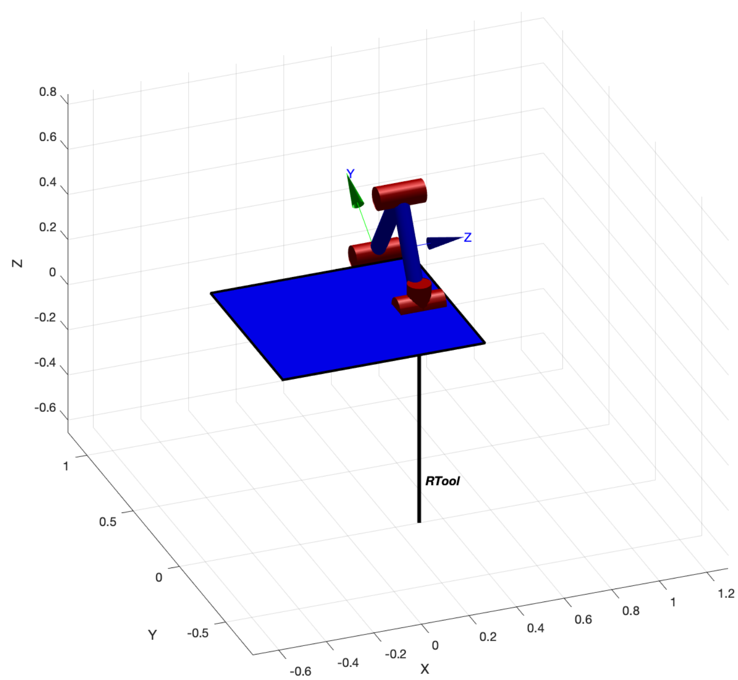

Figure 6: Navigation
$\boldsymbol{x}_{sto}$ = [0.1 0.4 0 0]
$\boldsymbol{q}_{sto}$ = [75.96 -24.76 54.47 0]

4 Jacobian

The Jacobian is a multidimensional form of the derivative, therefore if the non linear system has the form:

$$\boldsymbol{Y} = \boldsymbol{F}(\boldsymbol{X}) \tag{9}$$

derivating using the chain rule we can obtain

$$\partial \boldsymbol{Y} = \frac{\boldsymbol{\partial F}}{\partial \boldsymbol{X}} \partial \boldsymbol{X} \tag{10}$$

and the Jacobian J is a matrix containing all the partial derivatives of $\boldsymbol{F}$ with respect to $\boldsymbol{X}$. Therefore in compact form is possible to write

$$\partial \boldsymbol{Y} = J(\boldsymbol{X}) \partial \boldsymbol{X} \tag{11}$$

and by dividing for an infinitesiamal time we get

$$\dot{\boldsymbol{Y}} = J(\boldsymbol{X}) \dot{\boldsymbol{X}} \tag{12}$$

Is important to underine how the Jacobian is a time-varying linear transformation. Usually in robotics is possible to write $\dot{\boldsymbol{Y}} = \boldsymbol{\chi}$ and $\dot{\boldsymbol{X}} = \dot{\boldsymbol{\Theta}}$ where $\vec{\chi}$ is a vector of linear and angular velocities written in an inertial frame, $\boldsymbol{\Theta}$ are the joint variables and the Jacobian is a function of the latter ones, $J(\boldsymbol{\Theta})$.

$$\dot{\boldsymbol{\chi}} = J(\boldsymbol{\Theta}) \boldsymbol{\Theta} \tag{13}$$

The Jacobian has dimension $m \times n$ where m is the dimension of the velocities and n the one of the joint variables. For the Kapvik manipulater, having only 4 joint variables, we need a down selection of velcoities we can control. Therefore deciding to control only the first three and last one of $\boldsymbol{\chi}$, we can neglet the forth and fifth row of the Kapvik's Jacobian. That is, the Kapvik is under-actuated. The full Jacobian has the structure:

$$\begin{bmatrix} \cos(\alpha)(L_1 \sin(q3+q4) + L_2 \sin(q4)) & L_1 \sin(q3+q4) + L_2 \sin(q4) & L_2 \sin(q4) & 0 \\ \cos(\alpha)(L_1 \cos(q3+q4) + L_2 \cos(q4)) & L_1 \cos(q3+q4) + L_2 \cos(q4) & L_2 \cos(q4) & 0 \\ -\sin(\alpha)(L_2 \cos(q2+q3) + L_1 \cos(q2)) & 0 & 0 & 0 \\ \sin(q2+q3+q4)\sin(\alpha) & 0 & 0 & 0 \\ \cos(q2+q3+q4)\sin(\alpha) & 0 & 0 & 0 \\ \cos(\alpha) & 1 & 1 & 1 \end{bmatrix}$$

where α is the offset angle defined by Table 1, q_i are the joint variables and L_i the joint length.

By neglecting the forth and fifth row of the Jacobian, we obtain a square matrix that can be inverted. By invertig the Jacobian we can pass from cartesian velocities to joint rates and find the singular point of the mnaipulator by taking it's determinant and imposing it equal to zero. So if the determinant tends to zero, the Jacobin in not anymore full rank and turns out to be singular In this type of configuration when the manipulator is at or close to a singularity, large joint velocities may occur, or degenerate directions may exist where end-effector velocity is not feasible.

5 Dynamical Equation

For the dinamical model we consider the Joint Space dynamical formulation as follows:

$$\boldsymbol{\tau} = \boldsymbol{M}(\boldsymbol{q})\,\ddot{\boldsymbol{q}} + \boldsymbol{C}(\boldsymbol{q}, \dot{\boldsymbol{q}})\,\dot{\boldsymbol{q}} + \boldsymbol{G}(\boldsymbol{q}) + \boldsymbol{F}(\dot{\boldsymbol{q}}) \tag{14}$$

where:

$\boldsymbol{M}(\boldsymbol{q})$ is the Joint Space Inertia Matrix (NxN)
$\boldsymbol{C}(\boldsymbol{q}, \dot{\boldsymbol{q}})$ is the Coriolis and centripetal accelerations contribution (NxN)
$\boldsymbol{G}(\boldsymbol{q})$ is the gravity force contribution (Nx1)
$\boldsymbol{F}(\dot{\boldsymbol{q}})$ is the Coulomb friction (Nx1)

These matrices and vectors are computed with the use of the Composite Rigid Body Algorithm, through the Newton-Euler iterative algorithm. By using selected $[\ddot{\boldsymbol{q}},\ \dot{\boldsymbol{q}},\ \boldsymbol{q}]$, we can decompose the contributions on the torques of each singular component, building the matrices.

5.1 The Newton-Euler algorithm

The Newton-Euler algorithm employs an iterative approach to the inverse dynamic problem, to determine the torque $\boldsymbol{\tau}$ generated by a $[\boldsymbol{q_j},\ \dot{\boldsymbol{q}}_{\boldsymbol{j}},\ \ddot{\boldsymbol{q}}_{\boldsymbol{j}}]$ input, through the dynamical model. We firstly do an iteration from the joint **1** to the joint $\boldsymbol{N}$ to determine the angular velocity $\boldsymbol{\omega}$ and the angular acceleration $\dot{\boldsymbol{\omega}}$ of each link:

$${}^{i+1}\boldsymbol{\omega}_{i+1} = {}^{i+1}_{i}\boldsymbol{R}\,{}^{i}\boldsymbol{\omega}_i + \dot{q}_{i+1}\,{}^{i+1}\hat{\boldsymbol{Z}}_{i+1}$$

$${}^{i+1}\dot{\boldsymbol{\omega}}_{i+1} = {}^{i+1}_{i}\boldsymbol{R}\,{}^{i}\dot{\boldsymbol{\omega}}_i + {}^{i+1}_{i}\boldsymbol{R}\,{}^{i}\boldsymbol{\omega}_i \times \dot{q}_{i+1}\,{}^{i+1}\hat{\boldsymbol{Z}}_{i+1} + \ddot{q}_{i+1}\,{}^{i+1}\hat{\boldsymbol{Z}}_{i+1}$$

$${}^{i+1}\dot{\boldsymbol{v}}_{i+1} = {}^{i+1}_{i}\boldsymbol{R}[\,{}^{i}\dot{\boldsymbol{\omega}}_i \times {}^{i}\boldsymbol{P}_{i+1} + {}^{i}\boldsymbol{\omega}_i \times ({}^{i}\boldsymbol{\omega}_i \times {}^{i}\boldsymbol{P}_{i+1}) + {}^{i}\dot{\boldsymbol{v}}_i]$$

$${}^{i+1}\dot{\boldsymbol{v}}_{\boldsymbol{c}i+1} = {}^{i+1}\dot{\boldsymbol{\omega}}_{i+1} \times {}^{i+1}\boldsymbol{P}_{\boldsymbol{c}i+1} + {}^{i+1}\boldsymbol{\omega}_{i+1} \times ({}^{i+1}\boldsymbol{\omega}_{i+1} \times {}^{i+1}\boldsymbol{P}_{\boldsymbol{c}i+1}) + {}^{i+1}\dot{\boldsymbol{v}}_{i+1}$$

$${}^{i+1}\boldsymbol{F}_{i+1} = m_{i+1}\,{}^{i+1}\dot{\boldsymbol{v}}_{\boldsymbol{c}i+1}$$

$${}^{i+1}\boldsymbol{N}_{i+1} = {}^{Ci+1}\boldsymbol{I}_{i+1}\,{}^{i+1}\dot{\boldsymbol{\omega}}_{i+1} + {}^{i+1}\boldsymbol{\omega}_{i+1} \times {}^{Ci+1}\boldsymbol{I}_{i+1}\,{}^{i+1}\boldsymbol{\omega}_{i+1}$$

We can now perform an inward iteration, from joint $\boldsymbol{N}$ to joint $\mathbf{1}$ to find the torques as:

$$^{i}\boldsymbol{f}_{i} = {}^{i+1}_{i}\boldsymbol{R}\ {}^{i+1}\boldsymbol{f}_{i+1} + {}^{i}\boldsymbol{F}_{i}$$

$$^{i}\boldsymbol{n}_{i} = {}^{i}\boldsymbol{N}_{i} + {}^{i+1}_{i}\boldsymbol{R}\ {}^{i+1}\boldsymbol{n}_{i+1} + {}^{i}\boldsymbol{P}_{\boldsymbol{c}i}) \times {}^{i}\boldsymbol{F}_{i} + {}^{i}\boldsymbol{P}_{i+1}) \times {}^{i+1}_{i}\boldsymbol{R}\ {}^{i+1}\boldsymbol{f}_{i+1}$$

$$\tau_{i} = {}^{i}\boldsymbol{n}_{i}\ {}^{i}\hat{\boldsymbol{Z}}_{i}$$

5.2 Forward dynamic

To solve the forward dynamic, we need to compute the matrices in eq (14).

We can compute each column of the Joint Space Inertia Matrix by neglecting the $\dot{\boldsymbol{q}}$ and components:

$$\boldsymbol{M}_{j} = \mathrm{NE}(\boldsymbol{q},\, \boldsymbol{0},\, \ddot{\boldsymbol{q}}_{\boldsymbol{j}}) \tag{15}$$

where $\ddot{\boldsymbol{q}}_{\boldsymbol{j}}$ is a zero vector with 1 as j-th element. The gravity is ignored to compute $\boldsymbol{M}(\boldsymbol{q})$ and the motor inertia is added on the diagonal scaled by the square of the gear ratio.

$\boldsymbol{C}(\boldsymbol{q}, \dot{\boldsymbol{q}})$ is found by neglecting $\ddot{\boldsymbol{q}}$, the gravity terms and the friction on the joints. Coriolis and centripetal effects are computed using their dependence on $[\dot{\boldsymbol{q}}_{\boldsymbol{i}}\ ,\ \dot{\boldsymbol{q}}_{\boldsymbol{j}}]$ and $[\dot{\boldsymbol{q}}_{\boldsymbol{i}}{}^{\boldsymbol{2}}]$

$\boldsymbol{G}(\boldsymbol{q})$ is found by neglecting both $\ddot{\boldsymbol{q}}$ and $\dot{\boldsymbol{q}}$ terms, the link gravity is taken into account into the Newton-Euler formulation by adding an upward linear virtual acceleration to the first link of the chain.

$$\boldsymbol{G}(\boldsymbol{q}) = \mathrm{NE}(\boldsymbol{q}{,}0{,}0) \tag{16}$$

Lastly, $\boldsymbol{F}(\dot{\boldsymbol{q}})$ is modeled through the Coulomb friction, accordingly scaled by the gear ratio η to obtain the friction seen by the output of the gearbox.

$$\boldsymbol{F}_{i}(\dot{\boldsymbol{q}}) = \begin{cases} \tau_{f}^{-}\eta & \dot{q}_{i} < 0 \\ \tau_{f}^{+}\eta & \dot{q}_{i} > 0 \end{cases} \tag{17}$$

6 Trajectory Generation

In order to generate a smooth trajectory that enables the manipulator to pass between several joint configurations we need to implement the trapezoidal method for each joint. This method takes its name from the shape of the velocity profile, i.e. a trapezoid. In order to obtain a smooth transition in joint position we need to divide the trajectory in three main parts.

- Parabolic
- Linear Linear
- Parabolic

where the first parabolic part has a positive acceleration ($\ddot{\theta}$), while the last parabolic part has a negative acceleration. The acceleration is fixed joint per joint. Therefore the equations used for the generation of the trajectory are, for the first parabolic part, starting with zero velocity and from a certain joint variable q_0

$$\begin{aligned} q(t) &= q_0 + \frac{1}{2}\ddot{\theta}t^2; \\ \dot{q(t)} &= \ddot{\theta}t; \\ \ddot{q(t)} &= \ddot{\theta}; \end{aligned}$$

For the linear part, the acceleration is zero, and the velocity at the end of the parabolic part must be equal to the one of the starting linear part, therefore:

$$\begin{aligned} q(t) &= q_0 + \ddot{\theta}t_c(t - \frac{t_c}{2}); \\ \dot{q(t)} &= \ddot{\theta}t_c; \\ \ddot{q(t)} &= 0; \end{aligned}$$

where $t_c = \frac{t_f}{2} - \frac{1}{2}\sqrt{\frac{(t_f^2\ddot{\theta} - 4(q_f - q_0))}{\ddot{\theta}}}$ is the duration of the parabolic time and t_f is the duration of the whole segment.
At last we have have parabolic region, where the equation are the same to the ones of the first part, but this time with negative acceleration. It is good practise not to use the limit acceleration of the motor joint, so the real one are scaled, that is, $\ddot{\theta} = 5 \times 10^{-3}|\ddot{\theta}|$.
In addition a control over the acceleration $\ddot{\theta}$ needs to be implemented in order to make feasible the trajectory. The control has the form

$$\ddot{\theta} \geq \frac{4(q_f - q_0)}{t^2} \tag{18}$$

where q_f and q_0 are the final and initial joint positions.

6.1 Usage of via points

In order to avoid collisions we need to insert via points in the trajectory. Here the via points for the trajectory of each joint.

6.1.1 Stowage to Navigation

Having said the zero configuration of angles is displayed in Figure 2, the initial pose of the manipulator is defined by the joint angles $\vec{q} = \begin{bmatrix} 0 & 90 & 0 & 0 \end{bmatrix}$, and the final pose i want to reach is defined by the inverse kinematics, so $\vec{q} = \begin{bmatrix} 0 & 40.37 & -83.58 & 0 \end{bmatrix}$ we can choose for each joint the following via points:

- $q_2 = 90 \quad 0 \quad 0 \quad 40.37$
- $q_3 = 0 \quad 0 \quad -83.58 \quad -83.58$

while we are neglecting q_1 and q_4 since they don't take part in the transfer.

6.1.2 Stowage to Sample Retrieval

For this pose change, we are again not using the first and forth joint, the initial pose is defined by $\vec{q} = \begin{bmatrix} 0 & 90 & 0 & 0 \end{bmatrix}$ and the final pose $\vec{q} = \begin{bmatrix} 0 & -74.81 & 97.22 & 0 \end{bmatrix}$. For such trajectory we have chose the following via points:

- $q_2 = 90 \quad 0 \quad 0 \quad -74.81$
- $q_3 = 0 \quad 0 \quad 0 \quad 97.22$

6.1.3 Sample Retrieval to Sample Transfer

This last pose change needs to have also the first joint moved. The initial pose is the of the Sample Retrieval $\vec{q} = \begin{bmatrix} 0 & -74.81 & 97.22 & 0 \end{bmatrix}$, keeping the tool in a secure fixed position in order not to lose the sample during the transfer. The final pose is above the sample collector, and the joint configuration is $\vec{q} = \begin{bmatrix} 75.96 & -24.76 & 54.47 & 0 \end{bmatrix}$. For this last trajectory we have chose the following via points:

- $q_1 = 0 \quad 0 \quad 0 \quad 75.96$
- $q_2 = -70.2 \quad -24.76 \quad -24.76 \quad -24.76$
- $q_3 = 97.22 \quad 54.47 \quad 54.47 \quad 54.47$

6.2 Final Remarks concerning the trajectory generation

It is important to underline that the tool remains fixed in its position while the transfer from one configuration to another. Only after the locking into sample retrieval configuration one can change the joint variable associated to the tool in order to scoop the terrain. Then the tool remains fixed to assure a safe transfer to sample collector, where after the manipulator is again in position, the tool

changes its joint angle to transfer the sample acquired.
The choice of via points were made in order to avoid main episodes of collisions, for example the configuration chosen for the first trajectory allows the third link of the manipulator to distend into position without touching the base of the Kapvik, while the points for the third one assure safe sample transfer.
The trajectory profiles are displayed under the control law section, in the trajectory following subsection. (Figure 9, 10, 12, 13, 15, 16, 17)

7 Control Law

Regarding the manipulator control laws, we may want to refer to the dynamical vectorial equation for a rigid body:

$$\boldsymbol{\tau} = \boldsymbol{M}(\boldsymbol{q})\,\ddot{\boldsymbol{q}} + \boldsymbol{C}(\boldsymbol{q},\dot{\boldsymbol{q}})\,\dot{\boldsymbol{q}} + \boldsymbol{G}(\boldsymbol{q}) + \boldsymbol{F}(\dot{\boldsymbol{q}}) \tag{19}$$

where τ are the torques, M is $n \times n$ the inertia matrix of the manipulator, V is $n \times 1$ vector of centrifugal and coriolies terms, G is a $n \times 1$ vector of gravity term and F is a $n \times 1$ vector modelling other the non rigid body effects like friction.
To ensure the control we can model the system using the model partitioning model, in such case we have that

$$\tau = \alpha\tau' + \beta \tag{20}$$

where τ is n vector of torques. We may choose:

$$\begin{aligned} \alpha &= \boldsymbol{M}(\boldsymbol{q}) \\ \beta &= \boldsymbol{C}(\boldsymbol{q},\dot{\boldsymbol{q}})\,\dot{\boldsymbol{q}} + \boldsymbol{G}(\boldsymbol{q}) + \boldsymbol{F}(\dot{\boldsymbol{q}}) \end{aligned}$$

with the servo law having the form

$$\tau' = \ddot{\boldsymbol{\Theta}}_{\boldsymbol{d}} + K_v\dot{\boldsymbol{E}} + K_p\boldsymbol{E} \tag{21}$$

assuming that $\boldsymbol{E} = \boldsymbol{\Theta_d} - \boldsymbol{\Theta}$, therefore the closed loop system is characterized by the error equation

$$\ddot{\boldsymbol{E}} + K_v\dot{\boldsymbol{E}} + K_p\boldsymbol{E} = 0 \tag{22}$$

One should notice how the gains are constants matrices and diagonal, therefore each equation decoupled from the others and the error system can be written as

$$\ddot{e} + k_{vi}\dot{e} + k_{pi}e = 0 \tag{23}$$

7.1 Encoder modelization

We modelized the error coming from the reading of the encoder with a normal distribution around $\boldsymbol{q}$, with a deviance of σ. To guarantee statistical reliability of the controller, we take into consideration a factor of 3σ for the error.

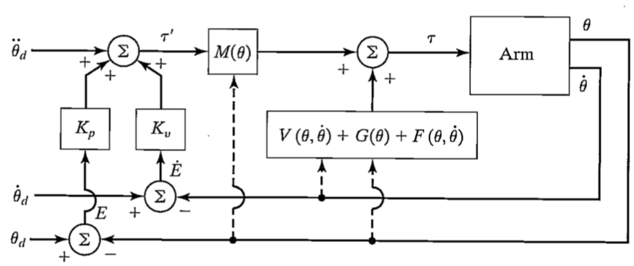

Figure 7: Control system scheme for a manipulator

7.2 Trajectory following

In order to follow a trajectory for each joint going from one configuration to another, we have the complete knowledge of the state of the joint variables, therefore the q_d , $\dot{q_d}$ and $\ddot{q_d}$ at every time step t. As previously explained we define the servo error as $e = q_d - q$ and the servo control law, for a single joint will be $\tau' = \ddot{q_d} + k_v\dot{e} + k_pe$. If in the system there is an initial error, it will be suppressed according to equation 19. For the sensor used in this report, the magnetic encoder has an accuracy of $\sigma = \pm 0.025°$.

7.3 From Stowage to Navigation

In order to control the trajectory from stowage to navigation we define the constants of the control and the accelerations. To stay in the constrains of the electric motor $\tau_m = 8.67[mNm]$ the input accelerations for both the trajecotry and the control system are not the maximum ones, bus pre-multiplied by a scaling factor. The constants are:

- $K_p = 100$
- $K_d = 2\sqrt{K_p}$ in order to obtain critical damping
- $\ddot{\theta} = 5 \times 10^{-3} \begin{bmatrix} 0.7168 & 0.7168 & 1.1360 & 0.8986 \end{bmatrix}$
- f = 100 Hz
- $\sigma = \pm 0.025°$
- $t_f = \begin{bmatrix} 45 & 35 & 30 \end{bmatrix}$

where the last item is the time that each joint spends to go from a via point to another.
In this pose change, only the second and third joint move, reminding that our zero pose has the configuration of the one in Figure 2, therefore the Stowage configuration will start from joint angles $\begin{bmatrix} 0 & 90 & 0 & 0 \end{bmatrix}$.

At the end of the trajectory the end effector must lock itself with the mast in order to obtain safe and steady navigation.

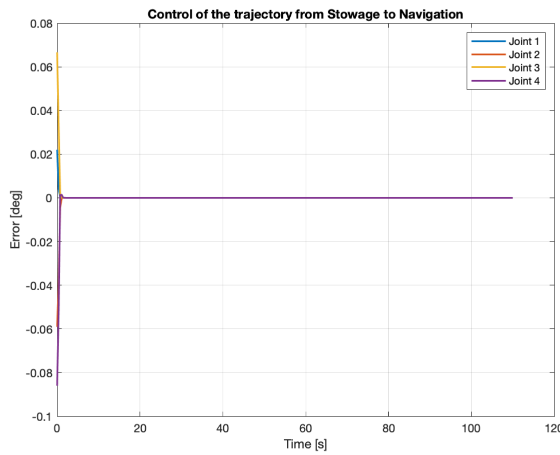

Figure 8: Stowage to Navigation control trajectory for each joint

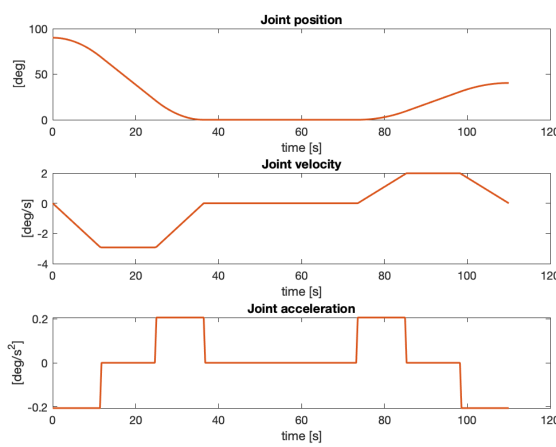

Figure 9: Stowage to Navigation second joint trajectory

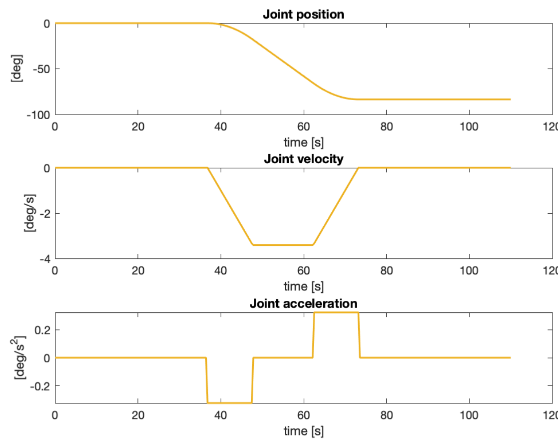

Figure 10: Stowage to Navigation third joint trajectory

7.4 Stowage to Sample retrieval

Having the same assumption made for the previous control trajectory, the control parameter for this pose change are:

- $K_p = 100$
- $K_d = 2\sqrt{K_p}$ in order to obtain critical damping
- $\ddot{\theta} = 5 \times 10^{-3} \begin{bmatrix} 0.7168 & 0.7168 & 1.1360 & 0.8986 \end{bmatrix}$
- f = 100 Hz
- $\sigma = \pm 0.025°$
- $t_f = \begin{bmatrix} 45 & 1 & 45 \end{bmatrix}$

and the plots:

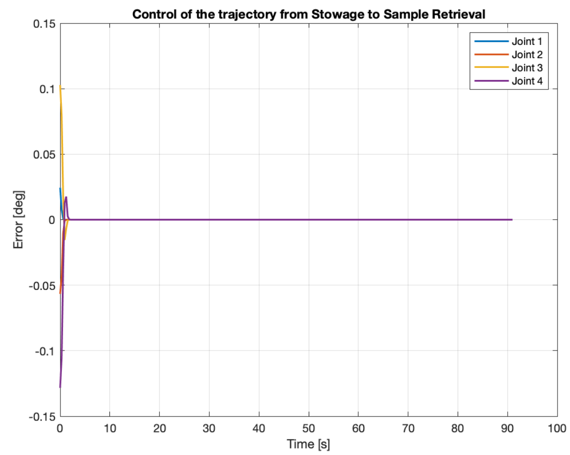

Figure 11: Stowage to Sample Retrieval control trajectory for each joint

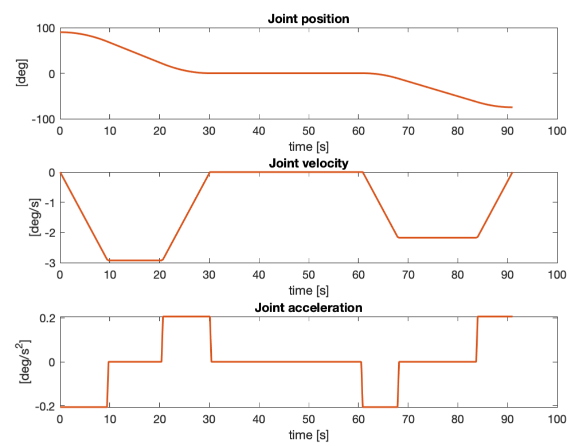

Figure 12: Stowage to Sample Retrieval second joint trajectory

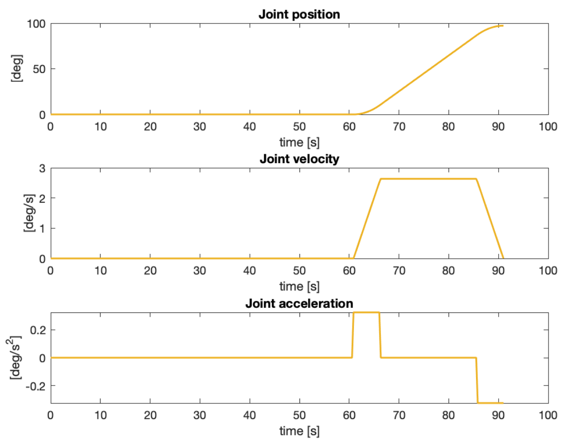

Figure 13: Stowage to Sample Retrieval third joint trajectory

7.5 Sample retrieval to sample transfer

Again we make the same assumption and define the parameters of the control. This time, due to the nature of the pose change, also the first joint needs to change its configuration, so this time we will move three out of four joints. In order to obtain a safe transfer, as already mentioned before, the tool must be locked in place in its configuration and then only after the trajectory has reached the final pose one can command the tool to leave the sample in the storage.
The control parameters are:

- $K_p = 100$
- $K_d = 2\sqrt{K_p}$ in order to obtain critical damping
- $\ddot{\theta} = 6 \times 10^{-3} \begin{bmatrix} 0.7168 & 0.7168 & 1.1360 & 0.8986 \end{bmatrix}$
- f = 100 Hz
- $\sigma = \pm 0.025°$
- $t_f = \begin{bmatrix} 30 & 1 & 40 \end{bmatrix}$

and the plots:

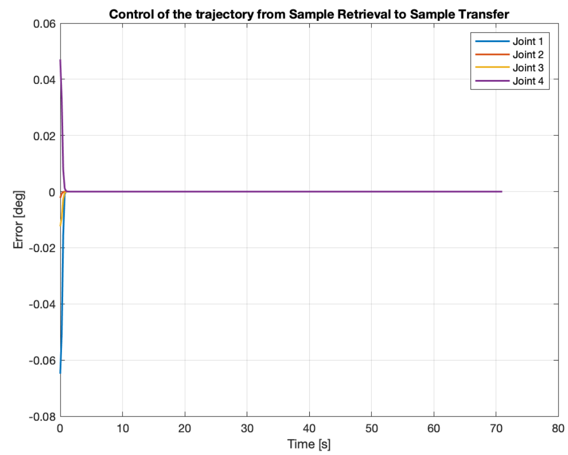

Figure 14: Sample Retrieval to Sample Transfer control trajectory for each joint

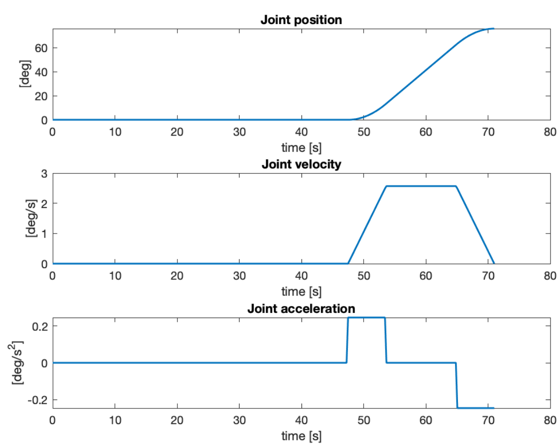

Figure 15: Sample Retrieval to Sample Transfer first joint trajectory

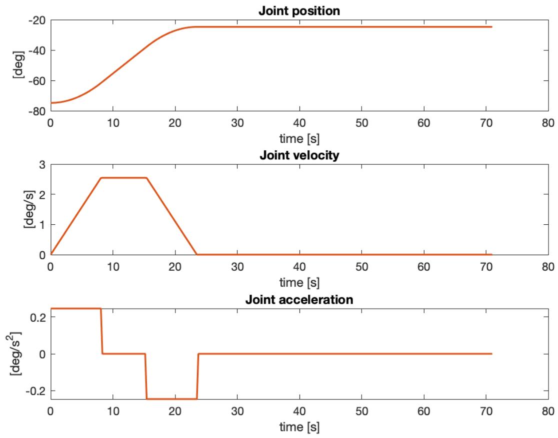

Figure 16: Sample Retrieval to Sample Transfer second joint trajectory

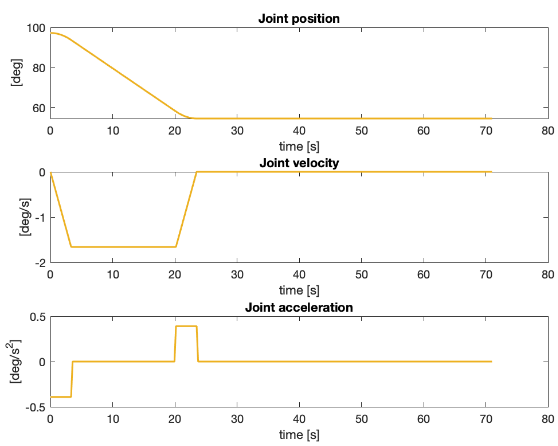

Figure 17: Sample Retrieval to Sample Transfer third joint trajectory